JOURNAL OF APPLIED ELECTROCHEMISTRY 27 (1997) 35–41

Indium as a cathodic material: catalytic reduction of formaldehyde

S. OMANOVIĆ, M. METIKOŠ-HUKOVIĆ

Department of Electrochemistry, Faculty of Chemical Engineering and Technology, University of Zagreb, Savska c. 16, PO Box 177, 10000 Zagreb, Croatia

Received 16 January 1996; revised 29 April 1996

The performance of indium as cathodic material for the electroreduction of small organic molecules is considered. The cathodic reduction of formaldehyde (FA) is an ideal model reaction for this purpose since indium has a very large overpotential for the hydrogen evolution reaction with and without FA. Kinetic sets of the reaction pathways, with respect to the Tafel slope and reaction order, are considered on the basis of quasi-potentiostatic measurements and cyclic voltammetry. The value of the Tafel slope $b_c \approx 60\,\text{mV dec}^{-1}$ indicates that the protonation of the adsorbed radical is the rate determining step in the proposed CECE mechanism. The reaction order with respect to FA is close to one in the limiting current regions but smaller in the Tafel region. The existence and kinetics of the radicals adsorbed during FA reduction are evidenced by very fast potentiodynamic experiments, with scan rates between 40 and $80\,\text{V s}^{-1}$. Electrochemical measurements are carried out on freshly *in situ* prepared In-electrodes. During cathodic polarization, the surface oxide film is reduced to In-metal via a solid-state mechanism. The crystallization kinetics of indium in the oxide matrix is also discussed.

List of symbols

A electrode surface area (m^2)
c concentration (M)
E electrode potential (V)
F Faraday's constant ($96\,500\,\text{A s mol}^{-1}$)
I current (A)
j current density (A m^{-2})
M molecular weight (kg mol^{-1})
n charge of metal cations
R resistance of external circuit (Ω)
t' anion vacancy
v scan rate (V s^{-1})

Greek letters
δ film thickness (m)
κ specific conductivity of the solution inside the film pores (S m^{-1})
η overpotential (V)
ρ film density (kg m^{-3})
σ roughness factor
θ fraction coverage of the electrode surface

Subscripts and superscripts
A anodic
C cathodic
CN metal nucleation
p peak
rev reversible

1. Introduction

There are many problems associated with the electroreduction of organic compounds on solid electrodes, especially in finding a good cathodic material that can catalyse the reactions and lead to the final product with the highest efficiency and lowest undesirable intermediate product formation. The electrochemical reduction of nitrobenzene is perhaps the most studied reaction in electroorganic chemistry [1, 2]. The reason for this is twofold: the complexity of the reduction and its importance in organic synthesis. The reduction of the nitrogroup, as well as many other organic molecules, is extremely sensitive to the effect of medium pH, nature of the medium, temperature, and the nature and structure of the electrode (cathode) material, particularly with respect to high overpotential for the hydrogen evolution reaction and the absence of the stable bridge-type complexes on the surface that can catalyse the hydrogen evolution reaction [3].

Among the organic fuels of technical interest, methanol offers the very attractive advantages of low cost and high energy efficiency. Prior to 1980, investigations were directed toward the development of methods for cheaper methanol production. One possible approach for methanol production from non-fossil sources was the electrochemical reduction of carbon dioxide [4]. A number of 5p metals (Zn, Pb, Sn, Cd and In) have been tested as cathodes for the electrocatalytic production of methanol from carbon dioxide with formic acid and/or formaldehyde as

0021-891X

the intermediate [5, 6], but the results showed that the conditions under which methanol can be prepared are limited. The highest faradaic efficiency (95%) in formic acid production from CO_2 electroreduction was obtained using an In electrode in an 0.5M Li_2CO_3 electrolyte and the highest efficiency for formaldehyde production was obtained in acidic solutions using a zinc amalgam cathode [7]. Ni, Cd, Pb, Cu, Ag, Al, Hg, Zn and Sn cathodes have been tested as electrocatalysts for the electroreduction of aliphatic aldehydes [8]. Dialcohols were found to be the principal products at solid and amalgamated electrodes as well as at mercury. For the reduction of propionaldehyde, Sn was found to be a more effective cathode than the other cathodic materials studied but the formation of Sn-organic surface complexes resulted in catalyst loss.

The reduction of formaldehyde has been studied on Sn, Pb and, extensively, in classical polarography [5, 9–12]. The results obtained on Sn and Pb electrodes showed that these metals are not suitable catalytic materials for FA reduction due to their tendency to form stable complexes with FA [13, 14] which act as a bridge between reactants in solution and the electrode surface, providing an alternative reaction pathway for the hydrogen evolution reaction (h.e.r.). This effect is specific in that only the rate of the hydrogen evolution reaction is increased, but not the rate of FA reduction [15]. In addition, both Sn and Pb catalyse the condensation of formaldehyde to form carbohydrates and similar polyalcohols [16] which block the electrode surface.

Unlike Sn and Pb, In and Hg do not form organic complexes with FA. This, and the fact that these metals have very large overpotentials for the h.e.r., with and without FA, made them potentially good catalytic materials for formaldehyde electroreduction reaction (i.e., methanol production). Investigations performed on indium electrodes showed almost 100% efficiency in methanol (production) and no mass loss of indium occurred during this process [5].

Previous studies on the electrochemical reduction of formaldehyde have shown that formaldehyde is predominantly in its electroinactive hydrated form, methylene glycol [5, 9–12]. In addition, there are small amounts of polyoxymethylene glycols, the concentration of which depends on formaldehyde concentration [16]. It is known that the limiting reduction current is governed by the reaction rate of methylene glycol dehydration to formaldehyde, which is the electroactive species. The overall reaction involves two electrons and the limiting current is controlled by a preceding reaction:

$$CH_2(OH)_2 \leftrightarrow CH_2O + H_2O$$

This dehydration appears to be a reaction catalysed by both base and acid. It was established [9, 12] that the mechanism of formaldehyde reduction is different in the pH ranges between 3 and 9 and above 9. The present paper is focused on the mechanism in the first range (Fig. 1).

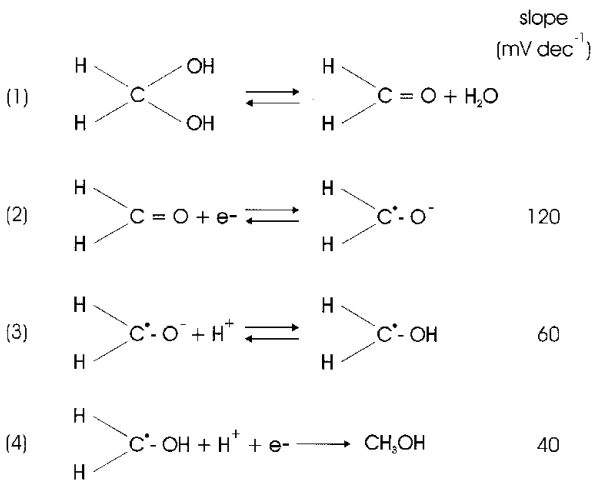

Fig. 1. Proposed CECE mechanism for the reduction of formaldehyde in solution pH 9 and expected values of the Tafel slopes b_c for each rate determining step under Langmuir adsorption conditions.

The purpose of this work was to study electrochemical reduction of FA on *in situ* prepared indium cathodes. Kinetic sets of the reaction pathway with respect to the Tafel slope and reaction order were considered. Formaldehyde reduction follows an electrochemically ideal type of model reaction, with electron and proton transfer, to form methanol with excellent yield [6].

2. Experimental details

All solutions were prepared from reagent grade chemicals and "conductivity water" (resistivity $> 6 \times 10^6\,\Omega$ cm). Solutions were deaerated by continuous bubbling with purified nitrogen. The buffer solution pH 9 contained 0.1M H_3BO_3 + NaOH and 0.9M KCl as the supporting electrolyte. The stock formaldehyde solution was prepared by diluting the concentrated (ca. 13M) reagent with the buffer solution to 1M. Actual formaldehyde concentrations were not checked by u.v. analysis or any other method. Working solutions were prepared by mixing the required amount of stock formaldehyde and buffer solution. In some experiments, formaldehyde solution was added to the electrolytic cell while the electrode was being polarized. Rapid mixing was achieved by vigorous nitrogen bubbling.

A standard three-electrode cell was utilized: the counter electrode was a platinum electrode and the reference electrode was a saturated calomel electrode (SCE) to which all potentials were referred. The working electrodes were prepared from spectroscopically pure indium foil, 0.5 mm thick (Aldrich), and sealed into a glass tube with epoxy resin. The exposed faces of the electrodes were 0.5 cm^2. In some experiments, the electrodes were chemically etched in a nitric acid–methanol bath. All measurements were performed at 23 ± 1 °C.

Electrochemical measurements were carried out on freshly prepared electrodes that were first cathodically polarized at −1.8 V in the working solution to remove

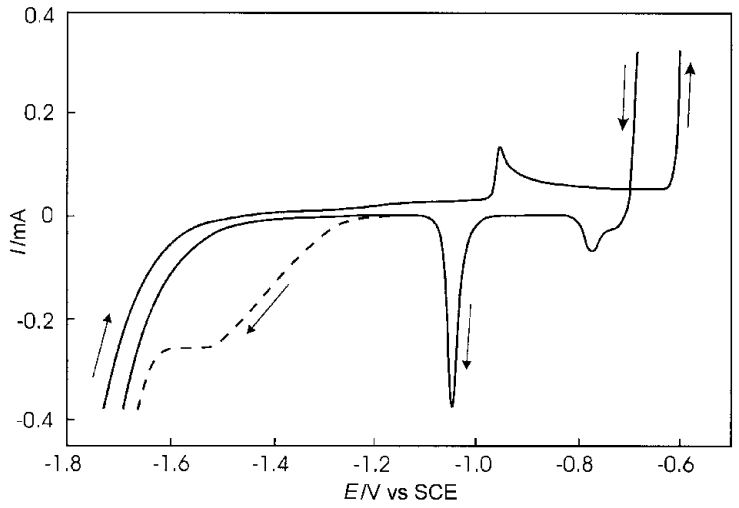

Fig. 2. Cyclic voltammogram of an indium electrode in (——) Na-borate + KCl buffer solution pH 9 and (– – –) with the addition of 0.1 M formaldehyde to basic solution. Scan rate: $v = 10\,\mathrm{mV\,s^{-1}}$.

any surface film. An EG&G PAR model 273 potentiostat/galvanostat controlled by a PC was used.

3. Results and discussion

3.1. *Kinetics of oxide film reduction and In-metal crystallization*

Figure 2 shows typical cyclic voltammograms obtained when freshly polished indium electrodes were introduced, under cathodic polarization at −1.8 V, into solutions with and without formaldehyde. In both cases, three characteristic potential regions could be distinguished during the anodic scan. In the first region, hydrogen evolution took place on the bare metal surface. At −1.0 V, the current showed a sharp maximum, which corresponded to the formation of an In(III)-oxide [17]. At more positive potentials, a low intensity steady current plateau was formed. In this region, the current was almost constant, indicating thickening of the passive oxide film with a constant electric field during linear polarization [18]. An abrupt current increase at −0.6 V corresponded to oxide film breakdown, due to the presence of chloride ions in the electrolyte solution. A distinct cathodic peak, observed in the returning scan, represented the reduction of the anodically formed In(III)-oxide layer directly to metallic indium. In the presence of FA (dashed line), the obtained curve was S-shaped with a limiting plateau after the cathodic peak. The appearance of a limiting current indicated that the process of formaldehyde reduction was under mixed activation-diffusion control. This will be discussed later. Figure 2 shows that the presence of FA in the basic solution increased the overpotential of the h.e.r. by about 800 mV.

The information on the kinetics of *in situ* electrodeposition of In-metal during oxide reductive decomposition, that is, the kinetics of In-metal nucleation (crystallization) in the oxide matrix, was obtained by studying the influence of the scan rate v on the cathodic current profile (Fig. 3), and cathodic potential limit variation $E_{l,C}$ on the anodic current profile (Fig. 4).

The anodic and cathodic peaks (Fig. 2) were characteristic of the processes of anodic indium oxide film

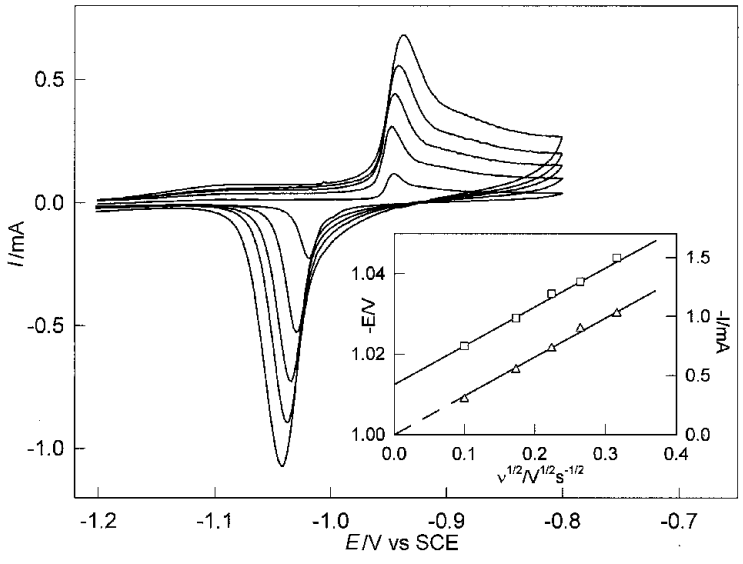

Fig. 3. Cyclic voltammograms of an indium electrode in Na-borate + KCl buffer solution pH 9 at different scan rates: $v = 10$, 30, 50, 70 and $100\,\mathrm{mV\,s^{-1}}$. Inset: Dependence of the (△) cathodic peak current and (□) peak potential on the square root of a scan rate.

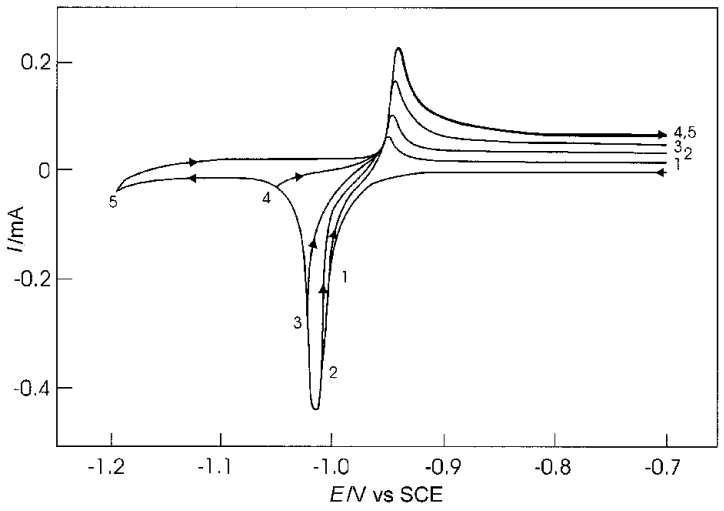

Fig. 4. Cyclic voltammograms of indium electrode in Na-borate + KCl buffer solution pH 9. The cathodic limit is variable. Scan rate: $v = 10\,\mathrm{mV\,s^{-1}}$.

formation and its reduction to metal, according to the equation:

$$2\mathrm{In(s)} + 6\mathrm{OH(aq)}^- \leftrightarrow \mathrm{In_2O_3(s)} + 3\mathrm{H_2O(aq)} + 6\mathrm{e}^- \quad (1)$$

The reversible potential for reaction (1) [19] is

$$E_{\mathrm{rev}} = -0.431 - 0.0591\ \mathrm{pH};\ \text{for pH 9},$$

$$E_{\mathrm{rev}} = -0.962\,\mathrm{V\,vs\ SCE} \quad (2)$$

The anodic and cathodic peak potentials, as well as the corresponding peak currents, changed with the scan rate. An increase in scan rate shifted the anodic peak to more positive potentials and the cathodic peak in the negative direction (Fig. 3).

The dependence of the cathodic peak current and potential on the square root of the scan rate $v^{1/2}$ is shown as the inset in Fig. 3. Under potentiodynamic conditions, the following equations described the scan rate dependence of the peak maximum [20, 21]:

$$I_{\mathrm{p}} = \left(\frac{nF\rho\kappa}{M}\right)^{1/2} A_0(1-\theta_{\mathrm{p}})v^{1/2} \quad (3)$$

$$E_{\mathrm{p}} = E_{\mathrm{O}} + \left(\frac{nF\rho\kappa}{M}\right)^{1/2}\left[\left(\frac{\delta}{\kappa}\right) + R_0A_0(1-\theta_{\mathrm{p}})\right]v^{1/2} \quad (4)$$

The cathodic peak current varied linearly with the square root of the potential scan rate, $v^{1/2}$ (Fig. 3). A linear dependence was also found between the peak potential E_{p} and $v^{1/2}$, which, when extrapolated to a zero scan rate, gave a spontaneous film reduction-potential E_0, that is, the potential of metal nucleation E_{CN}. With no polarization, this potential value is most suitable for comparison with thermodynamic data. The experimental value of $E_0 = -1.011\,\mathrm{V}$ is in very good agreement with the equilibrium potential E_{rev} calculated from Equation 2. The difference between the experimental value E_0 and the theoretical value E_{rev} gave a cathodic overpotential: $\eta = 49\,\mathrm{mV}$.

The relation between the cathodic peak potentials and peak currents of the voltammograms presented in Fig. 3 was found to be linear, with a slope expressed as a resistance, $R = \mathrm{d}E_{\mathrm{p}}/\mathrm{d}I_{\mathrm{p}} = 27\Omega$. The former showed that the reduction of In-oxide film was a solid state decomposition process leading to the In-metal crystallization (nucleation) and the spreading of In-metal nuclei to the covering of the whole electrode surface which was limited by resistance in the pores between the deposited metal sites [22].

Surface coverage with the newly formed metallic indium, θ_{p}, determined according to Equation 3, was 0.9999. The following values were used to calculate the surface coverage after the cathodic peak(s): $\rho = 7.3\,\mathrm{g\,cm^{-3}}$, $\kappa_{\mathrm{KCl}} = 0.112\,\mathrm{S\,cm^{-1}}$, $M = 114.82\,\mathrm{g\,mol^{-1}}$, $A_0 = 0.5\,\mathrm{cm^2}$ and $\sigma = 2$.

Further information about In-metal cyrstallization kinetics was obtained from the experiment presented in Fig. 4. The dependence of the anodic current profile on the cathodic potential limit $E_{1,\mathrm{C}}$ for an electrode passivated at $-0.7\,\mathrm{V}$ is shown. The cathodic sweep was reversed at various phases of the partial oxide reduction, marked as $E_{1,\mathrm{C}}$ (1, 2, ..., 5). On subsequent reanodization, the curve shape remained unchanged, but the anodic current was increased by the amount proportional to the area of the new metal surface surrounded by the unreduced oxide film. The results indicated that the cathodic current contribution at the potential positive and potential negative to the cathodic peak was related to the partial and complete In_2O_3 transformation into indium metal, (Equation 1). The newly reduced indium metal should therefore be on the outer surface of the oxide film (i.e., at the oxide/electrolyte interface) [23–25]. From the *in situ* impedance spectroscopy measurements [23], it was concluded that the mechanism of the In_2O_3 film reduction occurs through the electronic transport from the underlying metal to the film/solution interface: $e^-_{(\mathrm{metal})} \rightarrow t'_{(\mathrm{surface})}$. Freshly produced metallic indium would initially appear at the surface in anion vacancies t', where electrons were likely to be trapped. These centres act as the nucleation sites which the indium atoms, diffusing across the surface collect. The reduction of the In_2O_3 film leads to a porous In-metal surface layer, because In_2O_3 occupies a greater volume than In metal. This increase of the surface roughness (surface area) increases the catalytic activity on In metal. The result is a decrease

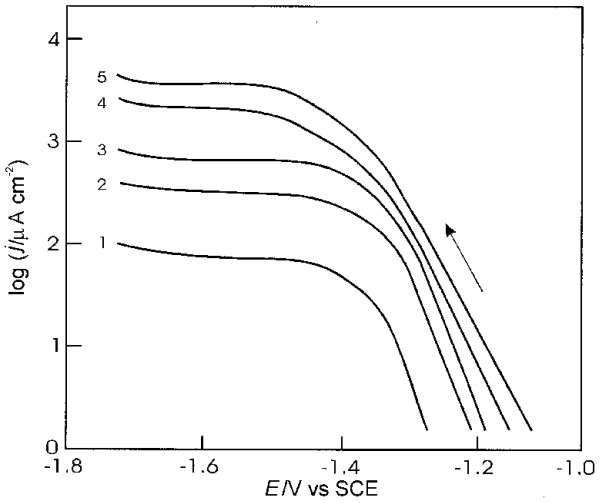

Fig. 5. Plots of current densities against potential for the reduction of formaldehyde on an indium electrode in Na-borate+ KCl buffer solution pH 9. Scan rate: $\nu = 1\,\mathrm{mV\,s^{-1}}$. Formaldehyde concentration: (1) 1×10^{-2} M; (2) 5×10^{-2} M; (3) 1.5×10^{-1} M; (4) 3×10^{-1} M; (5) 4×10^{-1} M.

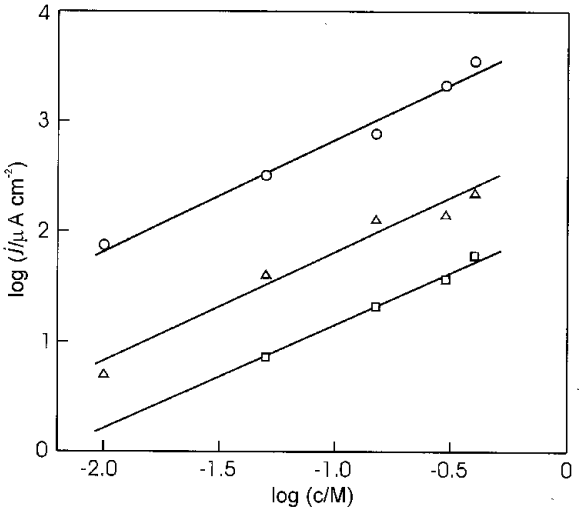

Fig. 6. $(\mathrm{d}\log j/\mathrm{d}\log c)_E$-reaction order for the formaldehyde reduction in the Tafel and limiting current regions obtained from the potentiodynamic polarization curves presented in Fig. 5. at potentials: (○) $E = -1.6$ V; (△) $E = -1.3$ V; (□) $E = -1.25$ V.

in overpotential (at a given apparent current density), an improvement in the operational characteristics of the In cathode for FA reduction.

3.2. *Formaldehyde reduction: quasipotentiostatic measurements*

A complex mechanism of formaldehyde reduction (Fig. 1) was investigated on the freshly *in situ* prepared In-electrode. The kinetic parameters, Tafel constant and reaction order were obtained.

Figure 5 shows polarization curves obtained with indium electrode in solutions containing various formaldehyde concentrations. Two characteristic regions can be observed at all the formaldehyde concentrations studied; a linear E–$\log j$ dependence, that is, Tafel region and a diffusion-controlled limiting current region. A linear E–$\log j$ relationship gave very reproducible Tafel slopes, the value of which depended on the formaldehyde concentration; with increase in formaldehyde concentration. Tafel slopes increase slightly from 60 mV decade^{-1} to 85 mV decade^{-1}. Considering the CECE mechanism proposed in Fig. 1, it seems likely that step 3 (i.e., protonation of the adsorbed radical) determines the reduction rate. The change in the Tafel slope was small enough to assume that the reaction mechanism and the r.d.s. do not change with the concentration. Larger values of the Tafel slopes obtained at higher formaldehyde concentrations could be attributed to the adsorption effects. Small amounts of polyoxymethylene glycols adsorbed on the electrode surface could influence the adsorption process and hence the Tafel slope through interactions with formaldehyde and/or its intermediates. As the rate constant for step 3 is coverage-dependent, a symmetry factor α in the Tafel relation has to be introduced [26] due to the change in adsorption energy with coverage. The symmetry factor depends on the electrolyte concentration in a progressive way as polyoxymethylene glycol replaces H_2O at the interface.

In comparison with the results obtained on In electrodes, the Tafel slopes on Hg electrodes were generally lower and were affected by pH changes [5, 12]. This was explained as a change in the r.d.s. of the reaction at higher pH values, from step 3 to 4 (Fig. 1). The change in the adsorption energy of the intermediate on its way from Hg to In probably increased the rate of step 4.

The reaction order with respect to formaldehyde was determined at a constant electrode potential from the slopes of $\log j$ against $\log c$ lines presented in Fig. 6. In the limiting current region, the calculated value of the reaction order was close to one over the whole concentration range studied. The values of the reaction order calculated in the Tafel region were between 0.98 and 0.78. This fractional reaction order indicated that the coverage of the electrode surface by formaldehyde or the intermediate species followed Langmuir–Temkin adsorption isotherm [27–29]. A similar but greater effect was observed on Hg electrodes [5, 12] and was attributed to the potential dependence of the coverage by intermediate electroactive or polymeric species.

3.3. *Formaldehyde reduction: cyclic voltammetry measurements*

The existence of the radicals adsorbed during FA reduction was demonstrated by fast potentiodynamic experiments. Figure 7 shows the results of cyclic voltammetry experiments performed in 0.2M formaldehyde solution at high sweep rates, 40 and 80 V s^{-1}. Small anodic and cathodic peaks were observed in each solution at sweep rates higher than the threshold value (40 V s^{-1}). The results of these experiments are in basic agreement with those of previous studies [5, 12, 30]. The cathodic and anodic peaks (Fig. 7) could

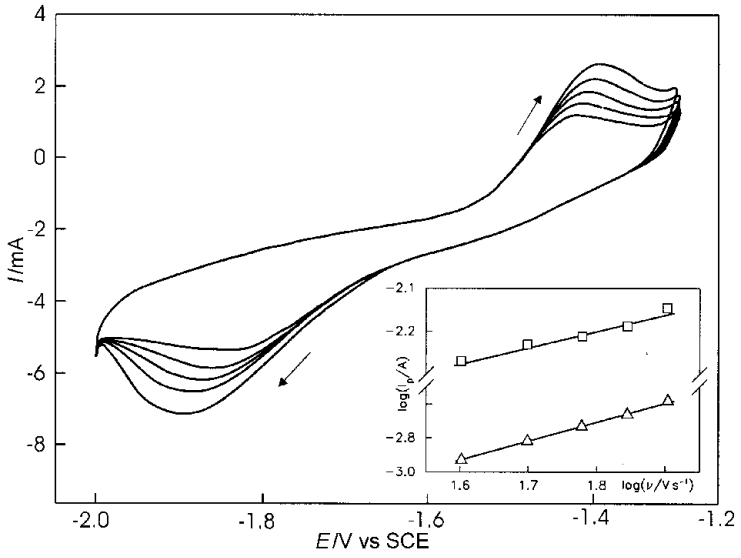

Fig. 7. Cyclic voltammograms of an indium electrode in 0.2 M formaldehyde solution pH 9 obtained with fast scan rates: $v = 40$, 50, 60, 70 and 80 V s^{-1}. Inset: log-log plot of the (□) cathodic peak current, and (△) anodic peak current against scan rate. (d log I_p^c/d log v) ≈ 0.5; (d log I_p^A/d log v) ≈ 1.0.

be attributed to the formation and oxidation of the anion radical intermediate. This behaviour is characteristic of an EC mechanism in which H^+ is involved in the following chemical reaction.

The log I_p–log v plot of the cathodic peak (inset in Fig. 7) shows a straight line with a slope of 0.5. The reaction of the radical intermediate formation is therefore diffusion-controlled through the mass transfer of bulk reactant under potentiodynamic conditions. Under quasipotentiostatic conditions, the apparent limiting currents were observed in the same potential region. The dehydration rate of methylene glycol is relatively slow at pH 9 and the amount of formaldehyde available for reduction could be considered constant during the time interval of the experiment carried out at fast sweep rates (40–80 V s^{-1}). The transfer of formaldehyde molecules across the interface region to the electrode surface thus results in a diffusion-controlled current.

For the anodic peak, the value of the log I_p–log v slope is about 1.0. The amount of intermediate available for oxidation appears to be no longer diffusion-controlled. Due to very high scan rates used in this experiment, it could be assumed that the reaction product formed during cathodic scan (resulting from the first electron transfer step) remains under the reaction sphere. This assumption is in accordance with the fact that step 3 (Fig. 1), is slow at pH 9 and anion radicals formed through step 2 have a sufficiently long lifetime for oxidation in the anodic sweep, during the time-interval of the experiment. Accordingly, the anodic scan exhibited only a kinetically controlled reaction. At a lower pH, step 3 was accelerated to such an extent that the anodic peak disappeared [12].

4. Conclusions

The performance of indium as the cathodic material for the electroreduction of small organic molecules was studied. The cathodic reduction of formaldehyde (FA) was an ideal reaction for that purpose since indium has a very large overpotential for the hydrogen evolution reaction with and without FA. The investigations were performed using the linear potential sweep technique (quasipotentiostatic measurements) and the cyclic voltammetry technique (potentiodynamic measurements).

The results indicated that formaldehyde was reduced on In fairly easily by the CECE mechanism, similar to that proposed for Hg. Kinetic sets of the reaction pathways were examined with respect to Tafel slope and reaction order. The value of the Tafel slope $b_c \approx 60$ mV dec^{-1} indicated that step 3 in the proposed mechanism, that is, protonation of the adsorbed radical, determined the reduction rate (r.d.s.).

The calculated reaction order with respect to formaldehyde was close to one in the limiting current region but less in the Tafel region. The fractional reaction order indicated that the coverage of the electrode surface by formaldehyde or the intermediate species was controlled by the Langmuir–Temkin adsorption isotherm.

Evidence for the existence of adsorbed radicals during formaldehyde reduction was obtained from fast potentiodynamic experiments. The observed cathodic and anodic peaks were attributed to the formation and oxidation of radical intermediates. The formation of radical intermediates was found to be a diffusion-controlled reaction, while their oxidation was kinetically controlled.

The kinetics of the crystallization of metallic indium in the oxide matrices was investigated *in situ* using the cyclic voltammetry technique. A solid-state mechanism for the reaction was proposed. The results showed that the indium metal nucleation potential lies close to the reversible potential for the reaction:

$$In_2O_3(s) + 6H^+(aq) + 6e^- \longrightarrow 2In(m) + 3H_2O(aq)$$

It was established that the electrcrystallization of In-metal in the oxide matrices occurred through electronic transport from the underlying metal to the film/solution interface: $e^-_{(metal)} \rightarrow t'_{(metal)}$. The newly

produced indium metal should be, therefore, on the outer surface of the oxide film (i.e., at the oxide/electrolyte interface). The growth of the indium metal nucleus and its spreading over the whole electrode surface occurred under ohmic resistance control.

References

[1] M. R. Rifi and F. H. Covitz, 'Introduction to Organic Electrochemistry', Marcel Dekker, New York (1974) p. 182.
[2] C. Ravichandran, M. Noel and P. N. Anantharaman, *J. Appl. Electrochem.* **26** (1996) 195.
[3] F. Haber, *Z. Elektrochem.* **4** (1898) 506.
[4] R. Roberts, R. P. Ouellette and P. N. Cheremisinoff, 'Industrial Applications of Electroorganic Synthesis', Ann Arbor Science Publishers, Michigan (1982) p. 100.
[5] P. G. Russel, N. Kovac, S. Srinivasan and M. Steinberg, *J. Electrochem. Soc.* **124** (1977) 1329.
[6] K. Ito, T. Murata and S. Ikeda, *Bull. Nagoya Inst. Technol.* **27** (1975) 369.
[7] T. V. Lysyak, Y. Y. Khuritonov and I. S. Kolomniltov, *Zh. Neorg. Khim.* **25**(9) (1980) 2562.
[8] B. G. Homiyakov, A. P. Tomylov and B. G. Soldanov, *Elektrokhimiya* **5** (1969) 848, 853.
[9] P. Valenta, *Collect. Czech. Chem. Commun.* **25** (1960) 853.
[10] O. R. Brown and J. A. Harrison, *J. Electroanal. Chem.* **21** (1969) 387.
[11] B. Barnes and P. Zuman, *ibid* **46** (1973) 323.
[12] S. Clarke and J. A. Harrison, *ibid.* **36** (1972) 109.
[13] J. D. Donaldson (edited by F. A. Cotton), 'Progress in Inorganic Chemistry', vol. 8, Wiley Interscience, New York (1967) p. 287.
[14] S. M. Kuronova, N. B. Grigorevand and N. Ya. Saveleva, *Sov. Electrochem.* **12** (1976) 973.
[15] S. Kapusta and N. Hackerman, *J. Electroanal. Chem.* **134** (1982) 197.
[16] J. F. Walker, 'Formaldehyde', Van Nostrand-Reinhold, New York (1974).
[17] S. B. Saidman and J. B. Bessone, *Electrochim. Acta* **36** (1991) 2063.
[18] S. Omanović and M. Metikoš-Huković, *Solid State Ionics* **78** (1995) 69.
[19] M. Pourbaix, 'Atlas of Electrochemical Equilibria in Aqueous Solutions', Pergamon Press, Oxford (1966).
[20] A. J. Calandra, N. R. de Tacconi, R. Pereiro and A. J. Arvia, *Electrochim. Acta* **19** (1974) 901.
[21] W. J. Müller, *Trans. Faraday Soc.* **27** (1931) 737.
[22] M. Metikoš-Huković, M. Šeruga and S. Ferina, *Ber. Bunsenges. Phys. Chem.* **96** (1992) 799.
[23] S. Omanović and M. Metikoš-Huković, *Thin Solid Films* **266** (1995) 31.
[24] D. Williams, *Electrochim. Acta* **21** (1976) 1097.
[25] M. Metikoš-Huković, *Electrochim. Acta* **26** (1981) 989.
[26] B. K. Conway and E. Gileadi, *Trans Faraday Soc.* **58** (1962) 2493.
[27] J. O. M. Bockris and B. E. Conway in, 'Modern Aspects of Electrochemistry', Butterworths, London (1964), chapters 3 and 4.
[28] S. Swathirajan, H. Mizota and S. Bruckenstein, *J. Phys. Chem.* **86** (1982) 2480.
[29] S. Swathirajan and Y. M. Mikhail, *J. Electrochem. Soc.* **138** (1991) 1321.
[30] S. Kapusta and N. Hackerman, *J. Electroanal. Chem.* **138** (1982) 295.